The Effect of EUV Molecular Glass Architecture on the Bulk Dispersion of a Photo-Acid Generator[*]

David L. VanderHart,[a] Anuja De Silva,[b]
Nelson Felix,[c] Vivek M. Prabhu,[a,†] and Christopher K. Ober[d,‡]

a)Polymers Division, National Institute of Standards and Technology, Gaithersburg, MD
b)Departments of Chemistry and Chemical Biology, c)Chemical and Biomolecular Engineering,
d)Materials Science and Engineering, Cornell University, Ithaca, NY

ABSTRACT

We have examined four molecular glasses (MGs) which are candidates for EUV photoresist formulations. These derivatized glasses, and their unprotected precursors, were investigated by both proton and ^{13}C solid state NMR techniques in the *bulk* state as pure materials and as mixtures with 5 or 10 % by mass of the photoacid generator (PAG), triphenyl sulfonium perfluorobutanesulfonate. The ^{13}C techniques gave information about crystallinity, purity, and the presence of the PAG. This paper characterizes the intimacy of mixing of the PAG and the MGs using proton spin diffusion methods. Phase separation of the PAG into PAG-rich larger domains was never seen; the PAG was always finely distributed. A maximum diameter for any PAG clustered into spherical domains was estimated to be 3.8 nm, which is too small to reflect thermodynamic incompatibility as the driving force during relatively slow removal of solvent. Hence, PAG blended samples are deduced to be thermodynamically compatible, with differential solubility in the preparation solvent the most likely candidate for producing the significant inhomogeneities in PAG concentration observed in a few samples. For one of the unprotected crystalline calix[4]resorcinarenes precursor materials, the solvent, N-methyl 2-pyrrolidinone (NMP) was used. The resulting solid was crystalline with a segregation of isomers, one of which formed a solid adduct with a 1:1 molecular ratio with NMP. Qualitatively, the strong NMP affinity for the calix[4]resorcinarenes is also evident in a) the immobility of the NMP, b) the fact that the ^{14}N quadrupolar interaction changes when NMP goes from the crystalline, unprotected host to a glassy, protected host, and c) that NMP tends to remain as a significant residue. Only the underivatized materials display crystallinity implying that the mixing of the PAG with any derivatized MG is not restricted by crystallization, at least not before the post-exposure bake step. As a final note, very strong hydrogen bonds exist in three underivatized materials which is reduced or eliminated with partial protection with t-BOC.

INTRODUCTION

It is clear that an intimate mixing of photoacid generator and matrix molecules is one key factor for good photoresist pattern development. It has further been proposed[1] that a smaller molecule, e.g. a molecular glass (MG) whose maximum dimension is, say, approximately 2 nm, could be used instead of a polymer as the matrix material. One motivational hypothesis is that a smaller molecule might form a surface with less roughness than a surface made up of larger molecules. The emphasis on glassy, rather than crystalline or semicrystalline materials seems obvious since the PAG would likely be excluded from any crystalline domains.

In this paper, solid state nuclear magnetic resonance (NMR) is used to investigate, both as neat and mixed materials, four MGs and one PAG in the bulk state. The material structures, names, stoichiometries and acronyms that we use are collected in Figure 1 and Table 1.

Table 1: Composition and abbreviations for each sample; see Figure 1 for basic chemical structures.

Sample Acronym	Main component [a]	t-BOC substitution level (% of orig. OH sites)	Mass % [b] (main)	Mass % [b] (minor) of TPS-PFBS
tBR-0	4tBPCR-0	0	100	
tBR-70	4tBPCR-70	70	100	
tBR-25	4tBPCR-25	25	100	
5tBR-70	4tBPCR-70	70	95	5
10tBR-70	4tBPCR-70	70	90	10
5tBR-25	4tBPCR-25	25	95	5
HR-0	4HPCR-0	0	100	
HR-70	4HPCR-70	70	100	
HR-25	4HPCR-25	25	100	
5HR-70	4HPCR-70	70	95	5
10HR-70	4HPCR-70	70	90	10
5HR-25	4HPCR-25	25	95	5
PB-0	HPB-0	0	100	
PB-100	HPB-100	100	100	
5PB-100	HPB-100	100	95	5
10PB-100	HPB-100	100	90	10
TS-0	BHEDBP -0	0	100	
TS-75	BHEDBP -75	75	100	
5TS-75	BHEDBP -75	75	95	5
10TS-75	BHEDBP -75	75	90	10

[a] Abbreviations and chemical correspondences:

TPS-PFBS = triphenylsulfonium perfluorobutanesulfonate, the photoacid generator (PAG).

t-BOC = *t*-butoxycarbonyl (t-BOC) [-C(=O)-O-C-(CH$_3$)$_3$] (replaces the hydroxyl hydrogen in protected molecules).

4tBPCR-n = 4-tertiary-butylphenyl calix[4]resorcinarene; "n" = percentage of t-BOC protection

4HPCR-n = 4-hydroxy-phenyl calix[4]resorcinarene; "n" = percentage of t-BOC protection

HPB-n = hexa[(*m*- and *p*-)phenol] benzene; "n" = percentage of t-BOC protection

BHEDBP-n = a "T"-shaped molecule: 4-[4-[1,1-Bis(4-hydroxyphenyl)ethyl]]-R,R-dimethylbenzylphenol; "n" = percentage of t-BOC protection

[b] These mass % values ignore impurity levels.

————

Calix[4]resorcinarenes ("HR" and "tBR" in Figure 1) have been used as both positive[2] and negative[3,4,] tone photoresists. Through *t*-BOC (t-butoxycarbonyl) protection of the hydroxyl groups, HR-0 and tBR-0 were converted into positive tone systems, HR-70 and tBR-70, respectively. The ring architecture of these resorcinarene systems is a key to attaining high glass transitions temperature (T_g) needed for lithographic processing. A variety of calix[4]resorcinarene derivatives can be formed[5] and the product is often mixture of stereo isomers.[5,6] For the resorcinarenes investigated herein, two stereoisomers are reported[6] for the HR-0 synthesis and one for the tBR synthesis. Mixtures of isomers can be used to promote the amorphous nature of these samples by preventing crystallization; hence, the reaction products were used without further purification, after removing residual solvent. Recent work by Ober et al. has reported sub 50 nm resolution using a molecular resist for calix[4]resorcinarene derivatives and employing EUV lithography.[7,8] The HR and tBR systems[9,10] were selected on the basis of their promising EUV lithography performance. Moreover, HR-70 showed an improved LER of 4.6 nm (3 σ) for 50 nm dense lines. These two structures also enable us to probe any differences in resist polarity since HR-70 has a polar hydroxyl functionality on each bridging phenyl ring, while tBR-70 has a non-polar t-butyl group. The protection level of 70 % of available sites in these two materials was found to optimize attributes such as adhesion, sensitivity for development, T_g and solubility in desirable spin-casting solvents. Lower t-BOC protection values (< 25 %) have also been added as a possible aid in understanding the miscibility effects during

deprotection. Though the exact distribution in the number of t-BOC groups on the resorcinarene molecules could not be analyzed the bulk protection ratio was confirmed through thermogravimetric analysis since the protecting group is driven off by heating.
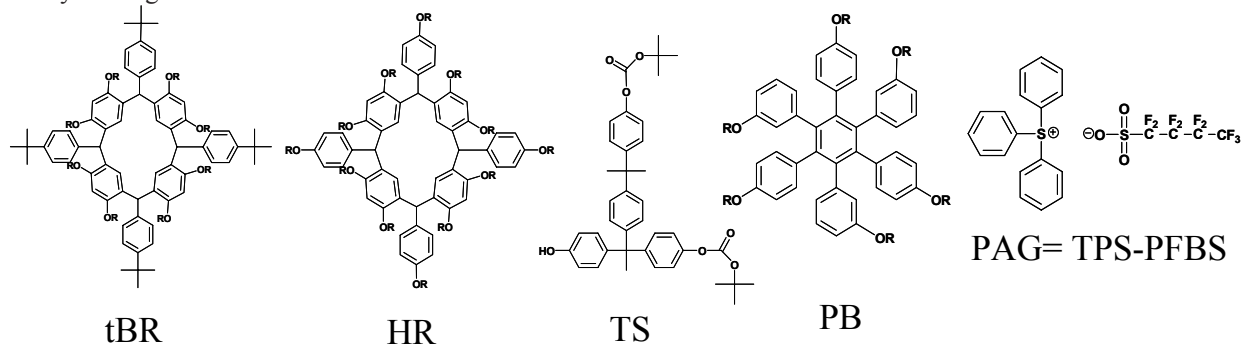

Figure 1. Basic chemical structures, with acronyms, for the materials used in this paper. (see also Table 1) Samples tBR-0, HR-0, TS-0 and PB-0 have R=H. Otherwise, the R groups are t-BOC groups, [t-butoxycarbonyl: i.e. -C(=O)OC(CH$_3$)$_3$], substituting at levels listed in Table 1. t-BOC structures are illustrated on the TS structure at two of the 3 available hydroxyphenyl sites. Note also that for HB, the substituents around the central phenyl moiety alternate with para and meta substituents. A second isomer is also present having one of the adjacent pairs in reverse order. These structural variations help to suppress crystallization of HB-0 and HB-100.

_____

In addition to the resorcinarene-based MG systems, other branched phenolic molecules have also evolved as successful MG resists. Some pioneering work in the Ober group has been based on commercially available systems such as the T-shaped (TS) molecule.[11] This material showed sub 100 nm patterning performance with both electron beam and EUV lithography. A main drawback in the T-shaped system was the low Tg (< 70 °C) upon partial protection with t-BOC groups. Hence, it served as a platform to design other high T$_g$ materials based on its branched phenolic architecture.

The first report on a chemically amplified resist system, made by Prof. Shirota and his coworkers, was based on the triphenylbenzene MG resist system.[12] In order to address the issue of low Tg in this triphenylbenzene system (Tg = 68°C), the Ober group designed a larger molecule with six phenolic groups attached to a central benzene moiety. This PB-0 sample was a structurally unique material with hydroxyl groups in alternating meta and para positions.[8] This molecule was obtained as a mixture of two isomers and hence resisted pi-pi stacking that leads to crystallization. Upon complete t-BOC protection, this molecule showed a high Tg of 105°C. This material has shown sub 50 nm resolution upon electron beam imaging with an all dry development using supercritical CO$_2$.[13]

The PAG chosen for this study, TPS-PFBS, is a commercially available PAG expected to have better environmental and safety characteristics compared to the commonly used PAG based on perfluorooctanesulfonate (PFOS).

Solid state proton NMR has been shown[14-18] to be a useful tool for probing the intimacy of mixing in blends of materials. The quantitative nature of proton signals and the high sensitivity of protons relative to other possible nuclei (e.g. ^{13}C) are important characteristics which direct us to techniques of proton observation. In particular the use of multiple pulse techniques, such as the MREV-8 sequence[19,20] provides a method of greatly narrowing spectra by eliminating dipolar interactions so that chemical shift effects dominate. The addition of magic angle spinning (MAS)[21,22] narrows spectra further so that, using the combined technique [23], CRAMPS (combined rotation and multiple pulse spectroscopy) spectra reflect the isotropic values of the chemical shift, just as is the case in liquid state NMR. Achievable resolution of about 1 ppm to 2 ppm, however, is only modest, compared to liquid state resolution, for most amorphous solids. Nevertheless, that resolution level is often sufficient for differentiating signals from chemically distinct spectral regions, i.e. aromatic and aliphatic protons in our case. We make use of the foregoing techniques in a multiperiod pulse sequence[15,17] in which the first fixed period is devoted to establishing a proton-polarization gradient between components and the ensuing variable "spin-diffusion" period is a time of full dipolar couplings where polarization is free to diffuse, approaching, in the case of good mixing, sample-wide spin equilibrium. An extended network of homonuclear dipolar couplings facilitates spin diffusion[24] which really is the diffusion of polarization and not of the spins themselves. Such spin

diffusion is an ongoing process; however, it is only detected in the presence of a polarization gradient. In the spin diffusion experiment, information about the intimacy of mixing of the components is extracted [25] from the behavior of the polarization as a function of this latter spin diffusion time, t_{sd}. The experiment which we do is analogous to a gedanken heat conductivity experiment applied to a solid mixture of two components. Imagine heating each component instantaneously to different average temperatures and then monitoring the temperature of each component as a function of time until a common temperature, not equal to ambient temperature, is reached. If one claims to know the thermal diffusivity of each component, then one can infer how intimately the components are mixed by the rate at which the common temperature is approached, provided that common temperature is reached in a time much shorter than the time required for regaining ambient temperature. In our case we instantaneously establish a proton-spin polarization gradient between the MG and PAG and then let "spin diffusion" take place. NMR signal strength, ratioed against the Boltzmann-equilibrium signal strength gives us a measure of spin "temperature".

We encountered a few major complications that render data gathering less than ideal, and we will mention them at the outset. First, our imposed polarization gradients are based on chemical shifts. Since the MGs have both aromatic and aliphatic protons (the PAG only aromatic), a strong initial polarization gradient is established both *within* the MG and *between* the protons of the PAG and the MG; however, it is only the latter, intermolecular equilibration that will tell us about MG/PAG mixing. Since we cannot separate the aromatic PAG signal from the aromatic MG signal, we cannot monitor the important *average* polarization of either the PAG or the MG until polarization gradients vanish for the MG. Since these protons are intimately and uniformly mixed into the chemical structure of the MG, we expect this 'intramolecular' process to be faster than the equilibration of the PAG/MG polarizations. However, if one really has intimate mixing of the components, it is clear that a lot of the early time information about the latter process will be masked by this blackout period and one will then be able to capture only the tail of the equilibration behavior. The second major complication in our study arises from the fact that in these mixtures, the fraction of total protons associated with the PAG is small (< 0.05). This means that one has to wait a longer time, i.e. adopt a more rigorous definition of intramolecular spin equilibration of the MG protons, so that any remaining changes in signal strength resulting from this type of equilibration are negligible with respect to the changes in PAG polarization. A final complication for a few of our samples is the existence of impurity components, such as residual solvents. In general, if these components are inhomogeneously distributed, and if there are sufficient numbers of associated protons, then, owing to limited resolution, we can get a result that looks like a poor distribution of PAG, when, in reality, it could be a poor distribution of the impurity.

As mentioned, we are looking at the general question of mixing of PAG and MGs *in the bulk state.* Photoresist applications are thin-film applications, not bulk-state applications. Therefore, we wish to be clear from the beginning that we are claiming to garner data that *necessarily* transfers to a given thin film preparation only for certain cases. The test we perform establishes (or fails to establish) the existence of intimate mixing of PAG and MG in the bulk state. The existence of such intimate mixing would signal a thermodynamic compatibility applicable to thin films as well. We claim this is a useful piece of information for thin film applications. Other issues to be considered in any comparison include the use of more volatile solvents for these samples, relative to those used in thin film applications and the related issue that if we see an inhomogeneous PAG distribution, it may be due to differential solubility of the PAG and MG in the solvent. This would be an ambiguous outcome since it may not apply to the solvent used in casting thin films, nor does that necessarily signal thermodynamic incompatibility. Finally, it is also clear that the bulk state does not permit any significant expression of surface-affinity effects which can occur in thin films.

EXPERIMENTAL
Materials. Synthesis of calix[4]resorcinarenes (HR-0 and tBR-0) and PB-0 [26] were performed at Cornell according to published reports.[5,8,10] TS-0 and TPS-PFBS were purchased respectively from TCI America and Aldrich; each was used as obtained. When referring to the TPS-PFBS loadings it will be implied as % by mass from this point forward, unless otherwise noted. The protection (or derivatization) of tBR-25 and tBR-70 followed literature procedures.[26] The protected samples were purified using column chromatography containing silica support (230-400 mesh) with acetone as the eluent. Purification of the protected compound is very important in removing minor impurities that affect thermal and lithographic properties of this material. HR-0 was not soluble in common organic solvents. Hence, 1-methyl-2-pyrrolidinone (NMP) was used as the reaction solvent for t-BOC protection. HB-25 and HB-70 samples were obtained via precipitation in water. The samples were then purified through column chromatography using acetone. Due to the high boiling point of NMP, some residual solvent was observed in the HR-25 and HR-70 samples even after drying in

vacuum overnight at 50°C. tBR-0 was easily soluble in common organic solvents; hence, t-BOC protection of this material was done in acetone. The products tBR-25 and tBR-70 were extracted with ethyl acetate and purified through column chromatography using acetone. TS-0 and PB-0 were protected according to literature procedures.[26] TS-75 was purified using an acetone column. PB-100 was purified using a CH_2Cl_2 column. NMR samples were all placed in the vacuum oven for at least 24 h at 40 °C prior to analysis.

NMR spectroscopy. NMR measurements were performed at NIST. All spectra were taken at ambient temperature. 300 MHz Proton spectra were taken using a Bruker Avance spectrometer[§] (Bruker Biospin, Inc., Billerica, MA) equipped with a low-proton-background CRAMPS probe manufactured by Doty Scientific, (Columbia, SC); the probe utilizes 5-mm-OD silicon nitride rotors. The proton radiofrequency power level gave nutation frequencies of 167 kHz (1.5 µs 90 ° pulses). The specific chemical-shift-based spin diffusion (CSBSD) experiment that we used has been described previously[17] as has its interpretation.[25] The MREV8 multiple pulse sequence[19,20] was employed with a 3.3 µs subcycle time leading to a 39.6 µs cycle time. Magic angle spinning rates were chosen to be 2525 Hz so that, in the initial stage of the CSBSD experiment where the magnetization gradients are prepared, the 10 or 20 MREV8 cycles used would correspond to exactly 1 or 2 periods of the rotor. This choice minimizes artifacts. Block averaging of spin diffusion spectra was employed in order to minimize the impact of any spectrometer drift.
For each sample, the Bloch-decay response to a single excitation pulse was also collected and Fourier transformed to give the normal broadline spectrum. Linewidths for the HR-0, PB-0 and TS-0 samples all were in the 30 kHz to 35 kHz range; however, the remaining samples had linewidths in the range from 13 kHz to 18 kHz owing to the contributions and numerical dominance of the motionally narrowed t-butyl protons of the t-BOC group. In addition to the Bloch-decay spectra, the longitudinal proton relaxation time, T_1^H, was also estimated from the zero-crossing time after in an inversion-recovery sequence.[27] Our interest in T_1^H was twofold. First, T_1^H relaxation competes with spin diffusion in producing intensity changes in the CSBSD experiment and we needed to know how competitive it is. All derivatized materials had T_1^H's in the range from 300 ms to 400 ms; underivatized materials had T_1^H's about twice as long. Hence, T_1^H processes, over the critical spin diffusion time of 7 ms contributed only a 2 % reduction in total intensity. Secondly, the measurement we conducted is capable of identifying the presence of multiple large (> 100 nm) phases (e.g. in HR-0) in the event that each phase has a different T_1^H. As magnetization recovers after inversion, the lineshape in the vicinity of the zero-crossing, if differing in anything but magnitude from the equilibrium lineshape, indicates the presence of multiple phases.

[13]C spectra were obtained on a non-commercial spectrometer operating at 2.35 T (25.2 MHz for ^{13}C and 100.2 MHz for protons). Cross polarization (CP) in combination with magic angle spinning (MAS) yielded CPMAS[28] spectra. The probe is non-commercial and included a MAS rotor/stator manufactured by Doty Scientific, Inc. Samples in 7-mm-OD zirconia rotors were spun at 4kHz, which was sufficient to keep all spinning sidebands out of the region of the centerbands in these spectra. Radiofrequency fields corresponded to nutation frequencies of 69 kHz for ^{13}C nuclei and 65 kHz for protons. Continuous-wave decoupling was used. The cross polarization time was 2 ms and usually 5000 to 10000 scans were collected for each spectrum.

Chemical shift scales for ^{13}C are referenced, by substitution, to the methine resonance of adamantane at 29.5 ppm and the proton shift scale for the CRAMPS spectra is referenced to tetramethylsilane at 0 ppm by substitution. Since small variations in rf-coil tuning for CRAMPS spectra can cause shifts, the uncertainty in the placement of the 0-ppm location is ± 0.5 ppm; for ^{13}C spectra, the corresponding uncertainty is ± 0.2 ppm.

Quoted uncertainties in measured quantities, unless otherwise specified, correspond to one standard deviation.

RESULTS AND DISCUSSION

Spin diffusion background and interpretation. First we define a couple of terms. *Polarization* is related to the ensemble-average projection, per spin, along the static field direction; in this paper, polarization will have a relative

---

[§] Certain equipment, instruments or materials are identified in this paper in order to adequately specify the experimental details. Such identification does not imply recommendation by the National Institute of Standards and Technology nor does it imply the materials are necessarily the best available for the purpose.

meaning where a polarization of 1.0 refers to the Boltzmann equilibrium polarization. *Magnetization* relates to the product of polarization times the number of spins. *NMR signal strength is proportional to magnetization* and, in the absence of T_1^H effects, *spin diffusion is an adiabatic process* that preserves the total magnetization. *Spin equilibrium* is that state where the polarization of all types of protons is the same. Boltzmann equilibrium is such an example. If a polarization gradient is imposed on a system, spin diffusion will allow polarizations to move diffusively, governed by spin diffusion constants, D (assumed known) until equilibrium is reestablished. If the diffusional process is too weak and those gradients cannot be removed in a time short compared to T_1^H, then it becomes more difficult to interpret any changes in terms of domain size.

To the extent that one can spectrally distinguish different types of protons in the sample, one can follow the rate of equilibration as a function of the spin diffusion time, t_{sd}. This is easier when distinct signals each correspond to one system component; it is more difficult, as in our case, when certain spectral components arise from multiple components. In our samples, we can distinguish signals arising from aromatic and from aliphatic protons based on chemical shift differences. While the PAG has only aromatic protons, the protected MGs have both. Since our initial imposed gradients are based on chemical shifts and can thus be thought of as aromatic/aliphatic gradients, we thereby accomplish the task of producing differences in average polarization between MG and PAG protons; however, we also have the complicating outcome that polarization gradients are generated *within* the set of MG protons. Since we cannot cleanly separate MG and PAG signals, we first have to wait for *intramolecular* spin equilibrium to be established on the MG molecules before we can monitor the behavior of the PAG polarization and isolate the *intermolecular* spin diffusion of most interest. Thus, we do a separate spin diffusion experiment on each MG and measure how long it takes for spin equilibrium to be reestablished (usually 3 ms to 4 ms in these cases). It is a disadvantage to forfeit knowledge of the early time data for the PAG. This early time behavior is often the most informative since it can be related directly[16,25] to interface area between PAG and MG; hence, for the data herein, we present a plausible way to project back to early times on the basis of observing only the longer-time behavior of PAG polarization.

Finally we make a few general comments about these experiments when the fraction of PAG protons in the sample is small (0.02 to 0.04 in most cases). First, any impurities can strongly influence the inferred spin diffusion behavior, especially if they are inhomogeneously distributed in the sample and contribute more protons than the PAG does. Second, consider the equation for calculating final equilibrium polarizations, P_f, when initial polarizations are known:

$$P_f = (M_\alpha + M_\beta)/(N_\alpha + N_\beta) \ = \ (P_{i\alpha}N_\alpha + P_{i\beta}N_\beta)/(N_\alpha + N_\beta) \tag{1}$$

where the M's are magnetizations, the P_i's are initial polarizations, the N's are the numbers of protons and α and β refer to each of the two components. Also consider the conservation of magnetization during spin diffusion, namely, that

$$\Delta M_\alpha = -\Delta M_\beta \quad \text{or} \ \Delta P_\alpha N_\alpha = -\Delta P_\beta N_\beta, \tag{2}$$

where the "Δx" quantities are respective differences between initial and final (or intermediate) values. When one proton fraction overwhelms the other, it is evident from the above equations that *the big polarization change is associated with the minor component* and that *the majority of that polarization change happens early in the process*, i.e. well before equilibrium is reestablished. As an example, suppose the proton fraction, $f_\alpha = 0.02$. Then, only the last 2 % of the PAG polarization change toward equilibrium would indicate whether the α component was mixed in more than 50 % of the β component. Hence, for our systems, this experiment is *insensitive to detecting modest variations* in PAG concentration throughout the MG. *Sensitivity in this experiment lies more in the following: a) detection of the presence of large (> 20 nm) PAG-rich regions when serious phase separation occurs* (e.g. for a fraction, f, of the PAG residing in a larger pure PAG phase, the range of observed change in PAG polarization during spin diffusion will be (1-f) times that expected for full equilibration) *and b) estimation of an upper limit for very small domain dimensions when the PAG is finely dispersed.* If spin equilibrium is not achieved in a two component system like this, one must consider the choice between fine-textured dispersal of PAG along with big concentration variations or a fraction of PAG in larger (> 20 nm) domains.

Spin Diffusion Spectra of Mixtures. Figure 2 is an example of a set of CRAMPS spin diffusion spectra obtained from the 10tBR-70 sample containing 10 % TPS-PFBS, where the CSBSD (chemical shift based spin diffusion[17]) has been employed. The initial polarization gradient formed in this experiment is a sinusoidally varying function across the proton CRAMPS spectrum. The figure caption describes the details and qualitative conclusions. Based on independent

measurements (not shown) on the tBR-70 sample, intramolecular spin equilibration will take 3 ms, so only lineshape changes for $t_{sd} \geq 3$ ms give information about PAG/MG mixing. In Figure 2, intermolecular spin equilibration does not change detectably after 7 ms, a time of the order of the intramolecular process; hence, one expects reasonably intimate mixing. Incidentally, a critical assumption upon which our analysis of any of these samples rests is that the PAG be present in an amount close to $\approx \pm 20 \%$ of the assumed stoichiometries in Table 1. Since we cannot separate the PAG and aromatic MG signals, we would like independent verification beyond the fact that all solids were carefully collected after preparation. Generally we could verify the PAG's presence to within $\pm 20 \%$ of expected using the aromatic intensity in the quantitative CRAMPS difference spectra (mixed sample minus unmixed sample). In cases where there was an excess of solvent impurity, we resorted to less quantitative ^{13}C spectra, where we relied on more strongly cross-polarizing, protonated, non-methyl carbon resonances for the analysis. In this way, we were able to verify the presence of PAG in all samples.
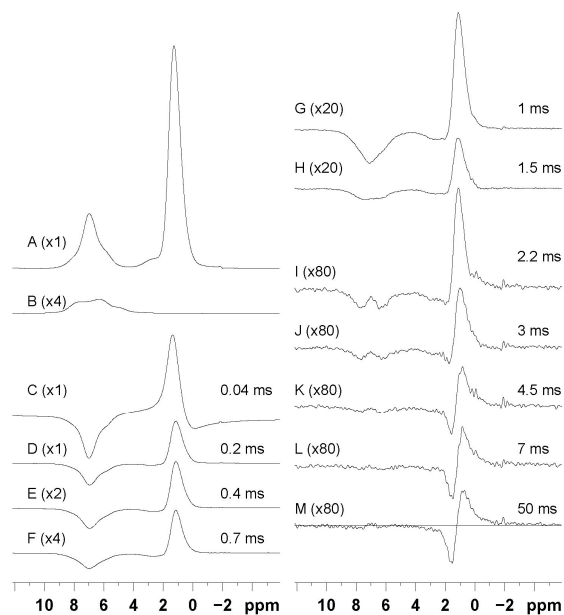

Figure 2: 300 MHz proton CRAMPS (combined rotation and multiple pulse spectroscopy) spectra related to spin diffusion of 10tBR-70. A: equilibrium lineshape; B: crystalline TPS-PFBS at a level 4 times that expected in 10tBR-70; C to M: "zero-integral" spin diffusion spectra at indicated spin diffusion times. Each latter spectrum is modified slightly from that experimentally obtained by adding a scaled amount of the 10tBR-70 equilibrium lineshape such that total integrals are zero (such spectral addition preserves gradients). Spectral multiplication factors are also shown. The aliphatic region is from about (0 – 5) ppm; the aromatic region is from about (6 – 9) ppm. The initial state features a negative aromatic polarization (arising from the MG plus the PAG) of much larger magnitude than the corresponding positive aliphatic polarization (MG only). Most of the initial intensity change over the first 3 ms is due to equilibration of aromatic and aliphatic protons in the 10tBR-70 component. Disappearance of intensity in these spectra means that sample-wide spin equilibration has been reached…true, within the signal-to-noise for the PAG protons after about 4.5 to 7 ms, thereby signaling intimate mixing of PAG and tBR-70. Apparent dispersive character of the aliphatic line is a known artifact of the method and arises from gradients in the static and radiofrequency fields; this artifact is larger for narrower lines, i.e. the aliphatic proton line associated with t-butyl protons. (The tBR-70 sample shows very similar behavior in this experiment.) The important issue is the simultaneously zero total integrals of both aromatic and aliphatic regions. Note the excellent sensitivity in these spectra.

_____

About spin diffusion plots. Quantitative analysis for spin diffusion spectra like that of Figure 2 has been discussed previously[18,29,30] and we will only mention a couple of key aspects. First, based on having done similar experiments on the pure components we have a good idea about the initial, average proton polarization levels for the aliphatic and aromatic protons in the experiment on the mixture. We use these levels as input, along with the data, in order to deduce the quantity, $\Delta M_s(t_{sd})$ as a function of the spin diffusion time, t_{sd}. Basically, $\Delta M_s(t_{sd})$ is a scaled quantity, proportional to the difference between the actual *average* PAG polarization and that final *average* PAG polarization characterizing the ideal state of full *spin equilibration of MG and PAG*. The scaling is such that if no spin diffusion between MG and PAG protons occurs (e.g. for complete phase separation into large domains) then $\Delta M_s(t_{sd}) = 1.0$. On the other hand, when complete spin equilibration between PAG and MG protons occurs, then $\Delta M_s(t_{sd}) = 0$. In all mixed samples we investigated, the major changes in $\Delta M(t_{sd})$ occur within the inaccessible first 3 ms; hence, rather than plot the tails of the data, it is a more precise to collect in Table 3 all values of $\Delta M_s(t_{sd})$ for 5 values of $t_{sd} \geq 3$ ms. The existence of impurities, as is true of some of our samples, represents yet another complication, especially if the impurity protons outnumber those of the PAG, since incomplete equilibration can also arise from the inhomogeneous distribution of the impurity.

The main conclusion to be drawn from the $\Delta M(t_{sd})$ values in Table 3 is that spin diffusion, at $t_{sd} = 3$ ms (where further *internal* spin equilibration within the MG should be small or negligible), has taken the PAG polarization through at least 85 %, and, most of the time, at least 92 % of the change required to reach sample-wide spin equilibrium. In other words, most of the major changes in PAG polarization occur over a time very similar to that required for intramolecular spin equilibration on the MG molecules. Furthermore, for those samples labeled in Table 3 as "intimately mixed", $\Delta M(t_{sd})$ is generally near 0.01 at $t_{sd} = 7$ ms. We now make the interpretation of data like that of Figure 2, more quantitative. Note in the 'remarks' column, there is a summary of key findings for all samples and some are complicated by trapped impurities. In particular, the samples showing the most sluggish approach to equilibrium, namely, 5HR-25 and, to lesser but similar extents, 5tBR-70, 5PB-100 and 10PB-100, each are summarized. In no case is there a strong argument for thermodynamic incompatibility; however, the PB-100 samples seemed to have consistent problems with differential solubility.

Estimate of PAG domain size for "intimately mixed" samples. One of the most informative portions of a spin diffusion plot is the initial slope in a plot of $\Delta M(t_{sd})$ vs. $(t_{sd})^{0.5}$, which slope we miss in our data. When initial gradients are spatially sharp, as they are in the scheme we use, the initial slope can be related to total interface area between PAG and MG, assuming, as we do, that the diffusion constants are known. Thus, we tried to relate the tails of our plots to the tails of another plot (where the whole curve was captured), and, by analogy, determine an approximate initial slope for our systems. Then, we go on to estimate, consistent with the reconstructed slope, the diameter, d_{PAG}, of a PAG spherical domain, assuming, as a worst case, that the PAG wants to phase separate. By this exercise we are trying to estimate, for those samples showing intimate mixing, to an accuracy of, say, $\pm$ 30 %, an upper limit to the size of PAG aggregation.

Earlier, while we were investigating mixing of the present PAG with polymeric matrices related to 193 nm photoresists, we obtained the unpublished data in Figure 3 showing the spin diffusion plot for a 95/5 blend of PHAdMA/TPS-PFBS (PHAdMA = poly(2-hydroxyadamantyl methacrylate). The big advantage of this system is that the only aromatic
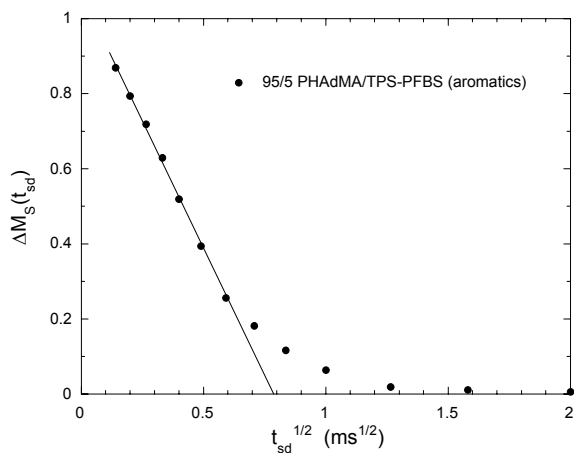

Figure 3. Spin diffusion plot for the 95/5 PHAdMA/TPS-PFBS system. The decay from 1 ms on to longer times mimics the average decay seen for the "intimately mixed" samples in Table 3, provided that the times indicated here are multiplied by a factor of 3. Uncertainties are given by the symbol size. The initial slope is the solid line and its intercept with the abscissa gives $(t_{sd}^*)^{0.5}$.

protons in this sample are the PAG protons; hence, the PAG polarization can be monitored at all spin diffusion times. When we compare the tail of this curve with those of the "intimately mixed" samples in Table 3, we find that comparable $\Delta M(t_{sd})$ values for our samples occur at t_{sd} values about 3 times longer than for the PHAdMA/TPS-PFBS mixture. The suggestion is therefore strong that the intercept of the initial slope with the abscissa, $(t_{sd})^{0.5}$, which is (0.79 ± 0.03) ms$^{0.5}$ in Figure 3, should be multiplied by $3^{0.5}$ to obtain $(t_{sd}^*)^{0.5}$ for our samples, i.e. $(t_{sd}^* = 1.88 \pm 0.15)$ ms. We can use this value to estimate the diameter, d_{PAG}, of a spherical domain of a very minor phase using the approximation[25]

$$d_{PAG} \approx 6(Dt_{sd}^*/\pi)^{0.5} \qquad , \qquad (3)$$

where D is an effective diffusion constant for the system. The diffusion constant we would ascribe[16] to the proton-rich, glassy PHAdMA, whose measured Bloch-decay proton linewidth is (48 ± 2) kHz, is 0.8 nm^2/ms. In contrast the corresponding linewidths of the blends under current investigation are all (14 ± 1) kHz, except for the lightly derivatized HR-25 and tBR-25 samples whose linewidths are (18 ± 1) kHz . The difference in linewidths between PHAdMA and

these MGs is mainly a result of the motional averaging of the preponderant t-butyl groups in our MGs. Exactly, the dependence of D on the matrix linewidth is debatable and depends on the detailed distribution of the protons; however, a reduction from that of PHAdMA by a factor of 2 is a conservative estimate and consistent with the length of time, 3 ms or 4 ms in our samples, for the intramolecular spin equilibration within the matrix molecules. This is at least a factor of 2 longer than in other glassy materials, e.g. poly(styrene),[30] whose linewidth is (35 ± 2) kHz and whose comparable intramolecular equilibration time is (1.4 ± 0.2) ms. Thus, by substituting $D = 0.4$ nm^2/ms (assumed applicable to both PAG and MG) into Equation 3, our estimate of the spherical diameter of any separated PAG phase, consistent with the observed tails of the spin diffusion curves, is $d_{PAG} = 2.9$ nm. Even if this estimate were off by 30 %, the maximum spherical diameter of any phase separated region would be 3.8 nm (containing 40 to 45 PAG molecules), i.e. still relatively small. To get some idea of the separation of domains implied by this upper limit, suppose the volume fraction of PAG was 0.04, and these domains were arranged on a regular body-centered cubic lattice, then the expected separation between the centers of the spheres would be about 10 nm. If estimates [31,32] of the PAG diffusion distance measured in other PAG/polymer photoresist systems are typical, a 5 nm diffusion radius is not small relative to those measured; hence, one would expect degraded photoresist performance if domains this large existed. Note also that 3.8 nm is a worst case spherical diameter for phase separation and we certainly cannot dismiss the other possibility that the PAG is dispersed on a molecular basis.

We now consider whether the formation of such a worst-case PAG-rich domain of diameter 3.8 nm is plausible. Given that these samples were formed by a modestly slow evaporation of the solvent, the idea that domains, rich in PAG and as small as 4 nm in diameter, would form based on some thermodynamic incompatibility, is implausible to us. Such small domains would have too much surface area and that would be too costly, energetically. Thermodynamic incompatibility should, in our opinion, lead to the establishment of much larger domains. Hence, we argue that *these experiments prove the thermodynamic compatibility of TPS-PFBS with those MGs in Table 3 which are characterized by "intimate mixing"*. The compatibility of this PAG with these and other systems we have studied, including fully aliphatic systems such as PMAdMA, is an intriguing subject in itself since the PAG is basically a salt and includes perfluorinated moieties as well as very polar moieties. So the interfacial energies would probably depend on the direction of approach of a matrix molecule to the PAG molecule. In this spirit, we emphasize that included in our concept of thermodynamic compatibility is the possibility that, rather than the PAG existing as isolated molecules, a few, fixed number of PAG molecules might cluster together for the purpose of lowering interfacial energies. Certainly, the experiments reported herein are not capable of proving or rejecting this possibility. However, in order to achieve the small domain size whose upper limit is 3.8 nm, a) the number of PAG molecules in such a cluster must be small and b) thermodynamics must *disfavor* the growth of larger, PAG-rich domains.

Table 3. Spin diffusion results for all mixtures of PAG and molecular glasses along with the theoretical fraction of PAG protons for each mixture based on the given stoichiometries.

Sample	Theor.[a] fraction of PAG protons	$\Delta M_s(t_{sd})$ [b]					Remarks (Abbreviations: **Ar/Al**: aromatic/aliphatic; **Eq**: equilibration; **SD**: spin diffusion; **inhomo**: inhomogeneous; **dist**: distribution; **imp**: impurity, **diff. sol.:** differential solubility in solvent)
		$t_{sd} = 3$ ms	4.5 ms	7 ms	10 ms	25 ms	
tBR-70							Ar/Al spin Eq. in 3 ms
5tBR-70	0.0186	.08	.06	.055	.044	.033	Inhomo dist of PAG/MG exists…diff.sol. likely, based on well behaved 10tBR-70; no NMP imp.
10tBR-70	0.0385	.053	.026	.014	.012	<.010	Intimate mixing
tBR-25							Ar/Al spin Eq. in 4 ms
5tBR-25	0.0190	.070	.020	<.010	<.010	<.010	Intimate mixing
HR-70							Ar/Al spin Eq. in 4 ms
5HR-70	0.0217	.064	.028	.018	.012	.008	Intimate mixing. NMP present at a level ≈
10HR-70	0.0448	.062	.035	.023	.014	.008	2 NMP molecules per 3 molecules of MG; NMP intimately distributed; also weak implied support for good mixing of the two types of derivatized isomers.
HR-25							NMP has (15 ± 3) % of total ^{13}C intensity; Ar/Al spin Eq. not quite fully reached; SD lineshape stabilizes at 7ms.
5HR-25	0.0247	.150	.102	.053	.039	.030	NMP has (12 ± 3) % of total ^{13}C intensity; Ar/Al spin Eq. not quite fully reached; three possible reasons for non-Eq.: a) inhomo dist of PAG/MG; b) inhomo dist of NMP, and c) some segregation in MG based on extent of derivatization. a) is considered least likely since HR-25 behaves similarly.
PB-100							Ar/Al spin Eq. in 4 ms
5PB-100	0.0217	.070	.053	.047	.042	.033	Negligible imp's; inhomo dist of PAG/MG exists; equal behavior of both samples points to likelihood of diff. sol. rather than thermodynamic incompatibility to explain inhomo dist of PAG.
10PB-100	0.0447	.066	.052	.045	.042	.035	
TS-75							Ar/Al spin Eq. in 3 ms
5TS-75	0.0194	.075	.032	.024	.010	.01	Intimate mixing for both samples
10TS-75	0.0402	---	.026	---	.012	---	

[a] Based on given stoichiometry in Table 1 and no impurities.

[b] $\Delta M(t_{sd})$ is the scaled deviation of aromatic PAG polarization from sample-wide spin equilibrium (see text). Its maximum range is from an initial value of 1.0 to 0.0, provided spin equilibrium is achieved. Standard uncertainties in each given value are ± 0.008 and ± 0.006, respectively, for the samples with 5 % and 10 % PAG.

NMP affinity for HR samples. A secondary issue that caught our attention in this investigation was the apparent affinity of NMP for crystalline HR-0. This sample showed two different domains having dimensions that exceeded 100 nm owing to the fact that each domain had a different longitudinal proton relaxation time, T_1^H. Figure 4 shows CRAMPS and ^{13}C spectra for HR-0 with decomposition into corresponding spectra associated with different domains. ^{13}C spectra identify the impurity as NMP and the CRAMPS spectra indicate a 1:1 adduct of NMP and HR-0 in the major phase. The fraction of the HR-0 associated with the major phase is 0.63 by this analysis, and, in view of reported[6] distribution (70/30) of the rccc/rcct isomers in the synthesis of HR-0, leads us to associate the adduct with the major symmetric rccc isomer. Incidentally, synthesis of the tBR-0 is included in this same report where only the rcct isomer is found.
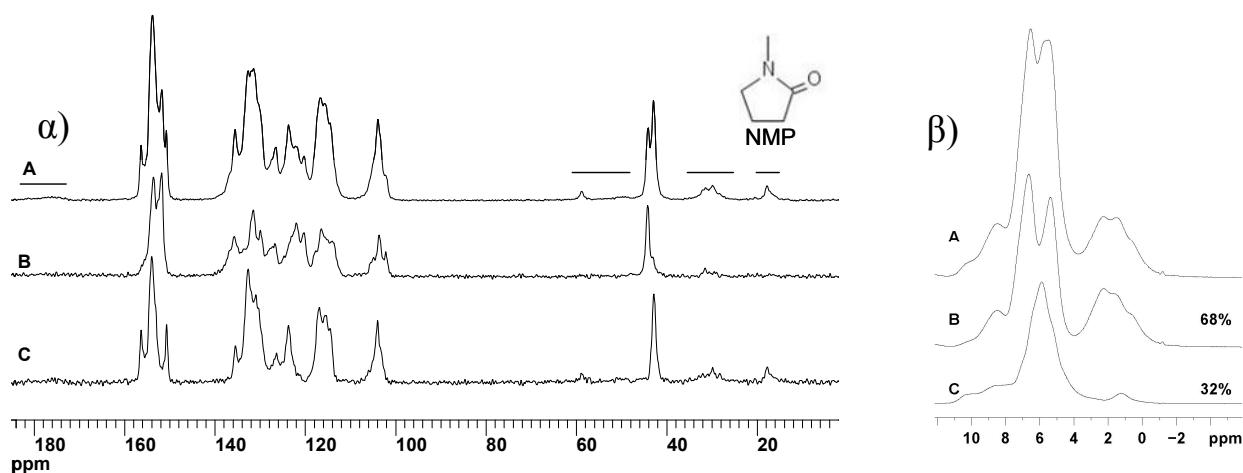

Figure 4: α): 25 MHz ^{13}C cross-polarization, magic-angle-spinning (CPMAS) spectra and β): CRAMPS spectra of HR-0. αA and βA are spectra of the total; αC and βB are component spectra for the majority phase and αB and βC represent the minority phase. This sample contains NMP whose resonance regions in α are indicated by the horizontal lines; NMP is responsible for the large aliphatic resonance (0 ppm to 5 ppm) in βA and βB. Analysis of aromatic/aliphatic intensity ratio in βB shows that this region is very close to a 1:1 molecular adduct of NMP and HR-0.

————————

The NMP was carried from the HR-0 through the protection reactions and subsequent cleanup procedures. Hence, we can surmise that the affinity of the NMP for the HR samples remains strong. However, the ^{13}C spectra give evidence that the interaction of NMP with the HR structure is different in the crystalline HR-0 and glassy HR-70 samples. This evidence comes by way of the shape of the NMP resonances for carbons bound to the ^{14}N atom (spin = 1) of the NMP heterocycle. The quadrupolar and Zeeman interactions of the ^{14}N atom compete in a way that causes an incomplete averaging under magic angle spinning of the ^{13}C -^{14}N dipolar interaction.[33-36] This incomplete averaging gives rise to generally asymmetric ^{13}C lineshapes. Substantial changes in the observed shape and width of the N-carbonyl and the N-methylene resonances point to a significant change, at least in the orientation, of the quadrupolar interaction within the NMP molecule between the crystal HR-0 sample and the glassy HR-70 sample. Figure 5 gives that spectrum.
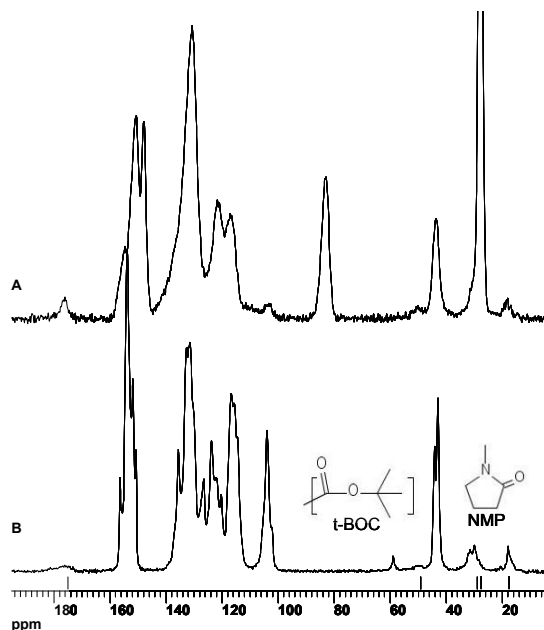
Figure 5. Comparison of CPMAS spectra of samples HR-70 (A) and HR-0 (B). Increase in linewidth from B to A is typical of going from an ordered, crystalline state to a disordered glassy state. In spectrum A one can identify resonances associated with t-BOC substituents (t-butyl methyls at 28 ppm, the quaternary ether carbon at 82 ppm and the carbonyl in the 145 ppm to 158 ppm range. Note also that a lot of shifting of aromatic intensity is seen in the range 100 to 125 ppm. Of particular interest is the change in lineshape for the NMP impurity resonances in the 50 ppm to 60 ppm region (the N-methylene resonance) and in the 170 ppm to 185 ppm region (the N-carbonyl resonance). Changes in these lineshapes indicate that the ^{14}N quadrupolar coupling of the NMP is changing, at least in orientation if not in magnitude, upon going from the crystalline, underivatized state of HR-0 to the glassy, derivatized state of HR-70 (see text). Positions of NMP resonances in chloroform solution are given by vertical bars above the shift axis.

Strong hydrogen bonding. Berglund[37] et al. have demonstrated a non-linear correlation of the isotropic chemical shift of protons involved in H-bonds with corresponding *inter*nuclear O…O distances. The correlations mainly involved acid protons, both organic and inorganic. Moreover, the correlation was monotonic, such that a reduction in O…O distance resulted in a shift downfield. Shorter H-bonds imply stronger interactions.

Figure 6 shows the CRAMPS spectra of the 10 unmixed samples. Of note are the downfield (8 ppm to 12 ppm) resonances of the HR-0, TS-0 and, to a lesser extent, the PB-0 and the HR-25 samples. From the correlation curve of Berglund,[37] resonances falling in this range, on average would correspond to O…O distances in the 0.30 nm to 0.27 nm range. Not all of the hydroxyl protons participate in these stronger H-bonds; the remaining are hidden under the aromatic resonances. From Figure 6 one would also conclude that the glassy t-BOC derivatives of HR and TS interfere with the formation of these stronger H-bonds since no such downfield resonances appear. Moreover, H-bonds which form in the tBR-0 sample are all of the weaker variety. One other observation, substantiated even more dramatically in the ^{13}C spectra, is that the best resolution is associated with the HR-0, tBR-0 and TS-0 samples. These samples are crystalline and all others are glassy.
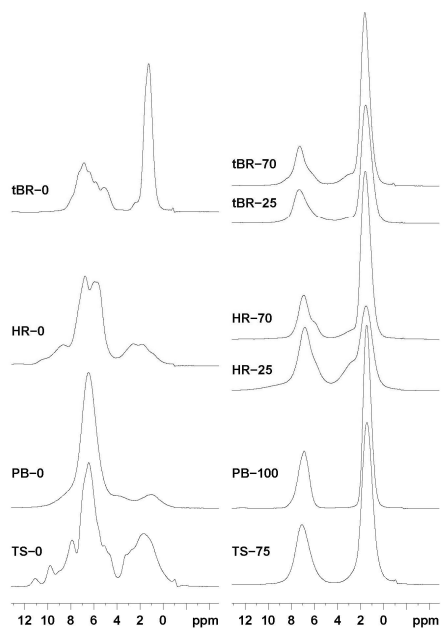

Figure 6. 300 MHz Proton CRAMPS spectra of all of the PAG-free samples. Downfield wings in the left column are indicative of strong H-bonding, for all but tBR-0. Left column, note the better resolution, supporting crystallinity, for all but PB-0. One can also see aliphatic resonances from the ethyl acetate in PB-0.

CONCLUSIONS

The photoacid generator, triphenylsulfonium perfluorobutanesulfonate, was blended with 4 molecular glasses (MGs), and the resulting, bulk glasses were analyzed by solid state NMR, with particular attention to the intimacy of mixing of PAG and MG. The MGs were all synthesized from precursors that had multiple phenolic moieties by the replacement of some fraction of the associated hydroxyl protons with t-butoxycarbonyl (t-BOC) groups. Proton spin diffusion methods were used to probe mixing in samples containing 5 % or 10 % PAG. Spin diffusion from the PAG protons to the MG protons was generally seen to proceed over times only a fewfold longer than the times required for equilibration between aromatic and aliphatic protons within the MG. The majority of samples were deduced to be "thermodynamically compatible" on the basis of a) interpreting the spin diffusion data as giving an upper limit of 3.8 nm diameter for any phase separated PAG domains (assumed spherical), and b) arguing qualitatively that thermodynamically driven phase separation is not consistent with the formation of such small domains since the tendency to minimize surface energies should lead to the formation of domains larger than 3.8 nm. Less than complete spin equilibration was seen in 4 samples and, for 3 of these, differential solubility in forming the bulk solid was suspected, rather than phase separation. In the fourth sample, 5HR-25, a) inhomogeneity in the distribution of a strongly associating solvent impurity or b) some segregation of the matrix based on differing levels of derivatization were considered more likely causes for the non-ideal spin diffusion behavior. Mass spectrometry methods are being pursued to characterize the distribution of derivatized molecules, which may provide further evidence for segregation based upon the polydispersity of protection.

These mixtures all have the property that the fraction of protons associated with the PAG is quite small and on the order of 0.02 to 0.04. In this range, besides giving an upper limit to domains when the system is mixed at a very intimate level, we could also easily identify any larger (> 20 nm) PAG-rich domains. These were not seen at any significant level. On the other hand, these experiments are not very sensitive to determining the *uniformity of concentration* for the finely dispersed PAG. One of the resorcinarenes, which consisted of two stereoisomers, was seen to have a special affinity for NMP such that the most symmetric isomer in the underivatized, crystalline parent material cocrystallized with NMP as a 1:1 adduct. The affinity of NMP persisted after t-BOC protection, however, the interaction between NMP and the parent isomer is different from the interaction between NMP and the derivatized MG in the sense that at least the orientation of the ^{14}N quadrupolar tensor on the NMP molecule changes. Such specific interactions may be critical in understanding base quencher additives retention and transport in such calixerane materials.

Finally, all derivatized products are glassy while 3 of the 4 underivatized materials are crystalline with the fourth, the hexaphenol benzene, probably showing 2-dimensional order. The underivatized samples, with the exception of tBR-0, all displayed some very strong H-bonds whose protons resonated downfield from the aromatic resonances. The protected MGs, however, had no strong H-bonds. On the basis of these measurements, we would surmise that each of these molecular glasses, in combination with this PAG do not exhibit phase separation provided that spin casting was done from a solvent having negligible problems with differential solubility. Interfacial segregation to substrate and surface in the case of thin films, however, is a separate issue. However, if deprotection went to completion it is possible for crystallization to take place leading to formation of very strong hydrogen bonding. This behavior may compromise rapid dissolution in an aqueous base developer. The inclusion of the tBR-25 and HR-25 samples was intended to probe whether there was a substantial change in compatibility of PAG and MG as one lowered the number of t-BOC substituents. These samples showed some compositional inhomogeneity; nevertheless, MG/PAG incompatibility in these samples is doubtful and was not shown.

ACKNOWLEDGEMENTS

References

[1] Yoshiwa, M., Kageyama, H., Shirota, Y., Wakaya, F., Gamo, K., and Takai, M.,"Novel class of low molecular-weight organic resists for nanometer lithography," Applied Physics Letters 69(17), 2605 (1996).

[2] Young-Gil, K., Kim, J. B., Fujigaya, T., Shibasaki, Y., and Ueda, M.,"A positive-working alkaline developable photoresist based on partially tert-Boc-protected calix[4]resorcinarene and a photoacid generator," Journal of Materials Chemistry 12(1), 53 (2002).

[3] Ueda, M., Takahashi, D., Nakayama, T., and Haba, O.,"Three-component negative-type photoresist based on calix[4]resorcinarene, a cross-linker, and a photoacid generator," Chemistry of Materials 10(8), 2230 (1998).

[4] Haba, O., Haga, K., Ueda, M., Morikawa, O., and Konishi, H.,"A new photoresist based on calix[4]resorcinarene dendrimer," Chemistry of Materials 11(2), 427 (1999).

[5] Tunstad, L. M., Tucker, J. A., Dalcanale, E., Weiser, J., Bryant, J. A., Sherman, J. C., Helgeson, R. C., Knobler, C. B., and Cram, D. J.,"Host Guest Complexation .48. Octol Building-Blocks for Cavitands and Carcerands," Journal of Organic Chemistry 54(6), 1305 (1989).

[6] Weinelt, F. and Schneider, H. J.,"Saarbrucken Series in Host-Guest Chemistry .27. Mechanisms of Macrocycle Genesis - the Condensation of Resorcinol with Aldehydes," Journal of Organic Chemistry 56(19), 5527 (1991).

[7] Yang, D., Chang, S. W., and Ober, C. K.,"Molecular glass photoresists for advanced lithography," Journal of Materials Chemistry 16(18), 1693 (2006).

[8] Chang, S. W., Ayothi, R., Bratton, D., Yang, D., Felix, N., Cao, H. B., Deng, H., and Ober, C. K.,"Sub-50 nm feature sizes using positive tone molecular glass resists for EUV lithography," Journal of Materials Chemistry 16(15), 1470 (2006).

[9] Bratton, D., Ayothi, R., Deng, H., Cao, H. B., and Ober, C. K.,"Diazonaphthoquinone molecular glass photoresists: Patterning without chemical amplification," Chemistry of Materials 19(15), 3780 (2007).

[10] Bratton, D., Ayothi, R., Felix, N., Cao, H. B., Deng, H., and Ober, C. K.,"Molecular glass resists for next generation lithography," Proceedings SPIE 6153, 61531D (2006).

[11] Dai, J. Y., Chang, S. W., Hamad, A., Yang, D., Felix, N., and Ober, C. K.,"Molecular glass resists for high-resolution patterning," Chemistry of Materials 18(15), 3404 (2006).

[12] Kadota, T., Kageyama, H., Wakaya, F., Gamo, K., and Shirota, Y.,"Novel electron-beam molecular resists with high resolution and high sensitivity for nanometer lithography," Chemistry Letters 33(6), 706 (2004).

[13] Felix, N. M., De Silva, A., Luk, C. M. Y., and Ober, C. K.,"Dissolution phenomena of phenolic molecular glass photoresist films in supercritical CO2," Journal of Materials Chemistry 17(43), 4598 (2007).

[14] Goldman, M. and Shen, L.,"Spin-Spin Relaxation in Laf3," Physical Review 144(1), 321 (1966).

[15] Caravatti, P., Neuenschwander, P., and Ernst, R. R.,"Characterization of Heterogeneous Polymer Blends by 2-Dimensional Proton Spin Diffusion Spectroscopy," Macromolecules 18(1), 119 (1985).

[16] K Schmidt-Rohr and H. W. Spiess,[Multidimensional SolidState NMR and Polymers], Academic Press, London, Chap. 13,(1994).

[17] Campbell, G. C. and VanderHart, D. L.,"Optimization of Chemical-Shift-Based Polarization Gradients in H-1-Nmr Spin-Diffusion Experiments on Polymer Blends with Chemically Similar Constituents," Journal of Magnetic Resonance 96(1), 69 (1992).

[18] VanderHart, D. L., Prabhu, V. M., and Lin, E. K.,"Proton NMR determination of miscibility in a bulk model photoresist system: Poly(4-hydroxystyrene) and the photoacid generator, di(tert-butylphenyl)iodonium perfluorooctanesulfonate," Chemistry of Materials 16(16), 3074 (2004).

[19] Rhim, W. K., Elleman, D. D., and Vaughan, R. W.,"Analysis of Multiple Pulse Nmr in Solids," Journal of Chemical Physics 59(7), 3740 (1973).

[20] Mansfiel, P., Orchard, M. J., Stalker, D. C., and Richards, K. H.,"Symmetrized Multipulse Nuclear-Magnetic-Resonance Experiments in Solids - Measurement of Chemical-Shift Shielding Tensor in Some Compounds," Physical Review B 7(1), 90 (1973).

[21] Andrew, E. R. and Lipofsky, J.,"Second Moment of Motionally Narrowed NMR-Spectrum of A Solid," Journal of Magnetic Resonance 8(3), 217-& (1972).

[22] Lowe, I. J.,"Free Induction Decays of Rotating Solids," Physical Review Letters 2(7), 285 (1959).

[23] Ryan, L. M., Taylor, R. E., Paff, A. J., and Gerstein, B. C.,"Experimental-Study of Resolution of Proton Chemical-Shifts in Solids - Combined Multiple Pulse Nmr and Magic-Angle Spinning," Journal of Chemical Physics 72(1), 508 (1980).

[24] A Abragam,[The Principles of Nuclear Magnetism], Oxford University Press, London, Chap. V,(1961).

[25] VanderHart, D. L. and McFadden, G. B.,"Some perspectives on the interpretation of proton NMR spin diffusion data in terms of polymer morphologies," Solid State Nuclear Magnetic Resonance 7(1), 45 (1996).

[26] Hansen, M. M. and Riggs, J. R.,"A novel protecting group for hindered phenols," Tetrahedron Letters 39(18), 2705 (1998).

[27] T. C. Farrar and E. D. Becker,[Pulse and Fourier Transform NMR], Academic Press, New York, pp.20-22(1971).

[28] Schaefer, J., Stejskal, E. O., and Buchdahl, R.,"High-Resolution C-13 Nuclear Magnetic-Resonance Study of Some Solid, Glassy Polymers," Macromolecules 8(3), 291 (1975).

[29] Rhim, W. K., Elleman, D. D., and Vaughan, R. W.,"Analysis of Multiple Pulse NMR in Solids," Journal of Chemical Physics 59(7), 3740 (1973).

[30] VanderHart, D. L.,"Proton Spin-Diffusion Studies of Polymer Blends Having Modest Monomer Size .1. Polystyrene Poly(Xylylene Ether), A Miscible Blend," Macromolecules 27(10), 2837 (1994).

[31] Jones, R. L., Hu, T. J., Lin, E. K., Wu, W. L., Goldfarb, D. L., Angelopoulos, M., Trinque, B. C., Schmid, G. M., Stewart, M. D., and Willson, C. G.,"Formation of deprotected fuzzy blobs in chemically amplified resists," Journal of Polymer Science Part B-Polymer Physics 42(17), 3063 (2004).

[32] Lavery, K. A., Vogt, B. D., Prabhu, V. M., Lin, E. K., Wu, W. L., Satija, S. K., and Choi, K. W.,"Exposure dose effects on the reaction-diffusion process in model extreme ultraviolet photoresists," Journal of Vacuum Science & Technology B 24(6), 3044 (2006).

[33] Frey, M. H. and Opella, S. J.,"High-Resolution Features of the C-13 Nmr-Spectra of Solid Amino-Acids and Peptides," Journal of the Chemical Society-Chemical Communications (11), 474 (1980).

[34] Naito, A., Ganapathy, S., and Mcdowell, C. A.,"High-Resolution Solid-State C-13-Nmr Spectra of Carbons Bonded to Nitrogen in A Sample Spinning at the Magic Angle," Journal of Chemical Physics 74(10), 5393 (1981).

[35] Olivieri, A. C., Frydman, L., and Diaz, L. E.,"A Simple Approach for Relating Molecular and Structural Information to the Dipolar Coupling C-14 N-14 in Cpmas-Nmr," Journal of Magnetic Resonance 75(1), 50 (1987).

[36] Zumbulyadis, N., Henrichs, P. M., and Young, R. H.,"Quadrupole Effects in the Magic-Angle-Spinning Spectra of Spin-1/2 Nuclei," Journal of Chemical Physics 75(4), 1603 (1981).

[37] Berglund, B. and Vaughan, R. W.,"Correlations Between Proton Chemical-Shift Tensors, Deuterium Quadrupole Couplings, and Bond Distances for Hydrogen-Bonds in Solids," Journal of Chemical Physics 73(5), 2037 (1980).